# Near-field properties of a gold nanoparticle array on different substrates excited by a femtosecond laser

**Nikolay N Nedyalkov**[1,2] **, Petar A Atanasov**[2] **and Minoru Obara**[1]

[1] Department of Electronics and Electrical Engineering, Faculty of Science and Technology,
Keio University, 3-14-1 Hiyoshi, Kohoku-ku, Yokohama 223-8522, Japan
[2] Institute of Electronics, Bulgarian Academy of Sciences, Tzarigradsko shousse 72,
Sofia 1784, Bulgaria

## Abstract

In this paper we present experimental and theoretical results on the properties
of the electromagnetic field in the near-field zone of gold nanoparticles
excited by an 800 nm ultrashort laser pulse. The near-field properties are
studied for the case of a single isolated particle and 2D nanoparticle array
case. Particles are deposited on different substrates: metal (Au),
semiconductor (Si) and dielectric ($SiO_2$). The calculations based on the finite
difference time domain (FDTD) simulation technique predict that the field in
the vicinity of the particles is enhanced as the magnitude of the field intensity
depends on the substrate material and the interparticle distance for 2D array.
For closely arrayed nanoparticles on the gold substrate, the maximal field
intensity is more than two times lower than that of a single particle. With the
increase of the distance between 200 nm diameter gold particles, the value of
the field intensity increases up to a distance of about 800 nm. The theoretical
prediction of the field enhancement on the substrate is confirmed
experimentally. The irradiation of the nanoparticles deposited on the three
different substrates with a single laser pulse of a Ti:sapphire laser results in a
nanohole formation. Discussion on the observed properties is presented.

## 1. Introduction

In the field of nanoscience and nanotechnology, the specific
properties of metal nanoparticles have attracted growing
attention in recent years [1–7]. Being an object of fundamental
physics as materials with 'unusual' properties related to
the size-dependent electron energy states, they also have
interesting applications in different areas of contemporary
technologies [2]. In noble metals, decrease of size down to
the nanometre range results in an intense peak in the extinction
spectra in the near-ultraviolet to visible region of the spectrum,
which is related to the resonant excitation of collective electron
oscillations (plasmons). The plasmon excitation can govern
the optical properties of the nanoparticles not only in the
far-field, but also in the near-field zone it can result in a
strong enhancement of the electromagnetic field [8]. Having
properties of an evanescent one, the enhanced field is localized
in the close vicinity of the particle, within a zone proportional
to the particle radius [9]. For a single isolated particle the
properties of the near-field depend on the particle parameters,
properties of the incident irradiation and the surrounding
medium. When a nanoparticle array is considered, these
properties can be additionally modified by the interparticle
plasmon coupling [10–13]. The narrow absorption spectral
band and the existence of the enhanced field in the vicinity
of noble particles opened a new innovative avenue in
biological applications as biomedical diagnostics [14], targeted
drug delivery [15], photo-thermal therapy [16] and surface-
enhanced Raman spectroscopy (SERS) [17]. The enhanced
optical field in the vicinity of the noble metal structure can also
result in a permanent modification of a substrate surface placed
in the near-field zone [6, 9, 18]. The recent advancement of
fabricating metal nanoparticles with a narrow size distribution
and methods developed for their arrayed deposition [19, 20]
opens a way for designing a processing technique that can
use the enhanced near-field for surface modification with a
spatial resolution governed by the size of the used particles.
Such a technique could satisfy the requirements of high

processing speed, low cost and application to a wide variety of materials that, despite of the developed different methods for precise nanostructuring [21–24], are not fully satisfied. Using a transparent nanoparticle array, several groups [25–28] demonstrated their efficiency in parallel nanostructuring of surfaces.

Although the far-field properties of noble particles and particle arrays are intensively investigated, the reports about the properties of the near electromagnetic field for these structures are rarely presented.

In this paper we report on the nanohole fabrication on different substrate materials produced by the enhanced near-field in the vicinity of gold nanoparticles irradiated by femtosecond laser pulses. The obtained results confirm the validity of the theoretical predictions and demonstrate that the use of the enhanced field can be an efficient tool for nanomodification. In order to bring this closer to an interesting application, we also present the near-field properties in the vicinity of arrayed nanoparticles, a system that is able to produce periodic nanostructuring on different substrate surfaces.

## 2. Experimental set-up

Gold spherical particles used in the experiment have a diameter of 200 nm, with a standard diameter deviation of less than 8% (BBInternational Corp.). The particles as a colloid are deposited on polished gold, silicon and glass substrates by a spin-coating method. Under the used conditions all the substrate surfaces are covered by randomly distributed gold particles. The RMS roughness of the virgin substrates (without particle deposition) is of the order of a few nanometres. The samples are irradiated by laser pulses delivered by a Ti:sapphire chirped pulse amplification system that produces pulses with energy of 1 mJ at a repetition rate of 1 kHz, and a centre wavelength of 800 nm. The laser pulse duration used is 100 fs FWHM. The laser radiation is incident normally to the substrate surface and it is focused by a lens with a focal length of 400 mm. The pulse energy is adjusted by a variable attenuator. The experiments are done in air on a single shot basis. The polarization of the incident irradiation is circular in the present experiment. The irradiated samples are analysed by SEM (Sirion 400, FEI Company). The substrate surface is not chemically cleaned after the laser irradiation. It should be mentioned that the incident laser intensity has a Gaussian profile which results in a different incident intensity corresponding to particles located at different positions within the focused laser spot. This results in different nanohole parameters within the irradiated area. The experimental data presented here are for the central area of the irradiated laser spot.

## 3. Simulation technique

To study near-field properties around the irradiated nanoparticles, a finite difference time domain (FDTD) simulation technique [29] is applied. The method is based on the numerical solution of the Maxwell's equations and can be used to obtain an adequate picture of the electromagnetic field distribution in the near-and far-fields around the structures with arbitrary shapes [30–32]. The simulation system consists of a
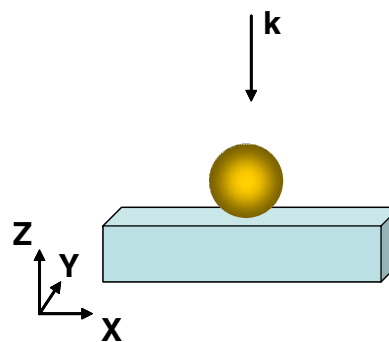


**Figure 1.** Schematic of the simulation system used in FDTD calculations. A gold particle is placed on a substrate. The incident electromagnetic wave propagates in the −*z* direction. For a 2D nanoparticle array a hexagonal arrangement is considered. The interparticle distance in this case is defined as the distance between the gold particle's centres.

(This figure is in colour only in the electronic version)

**Table 1.** Dielectric functions of the materials used in the calculations at a wavelength of 800 nm. The data are taken from [33] and [34].

| Dielectric functions | | |
|---|---|---|
| Au | Si | SiO$_2$ |
| $-24.016 + i1.510$ | $13.6 + i0.04$ | 2.365 |

gold nanoparticle or 2D nanoparticle array placed on different substrates. Figure 1 shows a sketch of the simulation system. Absorbing boundary conditions are applied on the boundary of the simulation cell. The optical properties (dielectric function) of the investigated materials used in the calculations are taken from [33] and [34] and are presented in table 1. For the simulations of the nanoparticle array, the effect of the interparticle distance on the near-field properties is investigated. The interparticle distance is defined as the distance between the centres of the particles. It is assumed that a hexagonal arrangement of the particles is placed on the array because this arrangement is predominantly obtained by the developed chemical methods for deposition [19, 20]. In all the simulations a circularly polarized wave irradiates the simulated system. Electric field strength of the incident wave is set at 1 V m$^{-1}$. The wavelength of the incident irradiation is 800 nm, corresponding to the ultrashort Ti:sapphire laser used in the experiment.

## 4. Results and discussion

### *Isolated particle*

In our recent work we demonstrated theoretically some properties of the near-field in the vicinity of a single gold nanoparticle irradiated by electromagnetic radiation [35]. In this configuration, the charge accumulation on the particle surface induces an image charge on the substrate surface. As a result, the formed electric field has a strong component in the direction perpendicular to the substrate surface. Due to the specific properties of the near-field, the zone of the highest field enhancement (ratio of the specific near-field to the incident field intensity) for the isolated particle is localized in the vicinity of the contact point between the particle and

the substrate, having a specific size smaller than the particle's diameter. Furthermore, the resulting near-field distribution can also be governed by the scattering and reflection on the electromagnetic field by the particle and substrate. Since the optical parameters and the induced charge on the substrate surface are functions of its dielectric properties, different field enhancement is obtainable for the different materials.

Figure 2 shows SEM images of holes produced on (a) Au, (b) Si and (c) SiO$_2$ substrate when the nanoparticles deposited on the substrate are irradiated by a single laser shot. The laser fluence is 0.1, 0.13 and 6.3 J cm$^{-2}$, respectively. In all cases, the incident fluence is lower than the threshold for native surface modification estimated by the single shot experiment. In the case of gold and silicon surfaces the laser fluence is about two times lower than the bulk modification threshold. For the case of glass substrate, the nanohole formation is clearly observed at laser fluence of about only 1.1 times lower than the threshold. The near electric field intensity calculated by the FDTD simulation is also shown with each SEM image in figure 2. The near electric field intensity is highest for the case of gold substrate while it is lowest for the glass one, an effect related to the value of the dielectric function of these materials. The ring shape structure of the 2D near field distribution can be attributed to some geometrical considerations. In the present simulations the incident radiation is perpendicularly incident to the substrate surface. The magnitude of the induced polarization of the particle decreases in the direction to the poles where it approaches zero. Furthermore, the magnitude of the near-field decreases rapidly with the distance from the particle surface. Thus, when a substrate is present, the induced charge density on its surface will be increased in the direction to the contact point between the particle and the substrate. As a result of these effects, the enhanced field will form an area with a ring shape for the case of a circular polarization of the incident laser.

A comparison between the calculated field distribution as an initial energy deposition pattern and the experimentally observed holes as a final result of the electromagnetic field–matter interaction, can be done by taking into account realization of complex processes. They may include local heating, melting, melt dynamic and ablation. The heating of the substrate in the vicinity of the nanoparticles can also result in a change of the local chemical composition of the substrate surface. It is seen, however, that the hole shape follows the symmetry of the zone with the highest field enhancement. Furthermore, the experiments performed with *linearly polarized* incident radiation show a direct connection between the direction of polarization and the hole shape. This effect is also confirmed by simulation [9, 35]. The observation of hole formation only near the threshold fluence for native glass surface modification can be explained by the low field enhancement predicted by the model simulation. The size of the formed dimple in this case is in good agreement with the size of the zone with the maximal near-field intensity value. This can be related to the fact that the heat conduction in the glass substrate is lowest among the used materials. In the case of metal substrate the redistribution of the incident energy by the free electrons and the effects related to the electron heat conduction can increase significantly the initial energy deposition region. These phenomena are important especially



a)



b)



c)
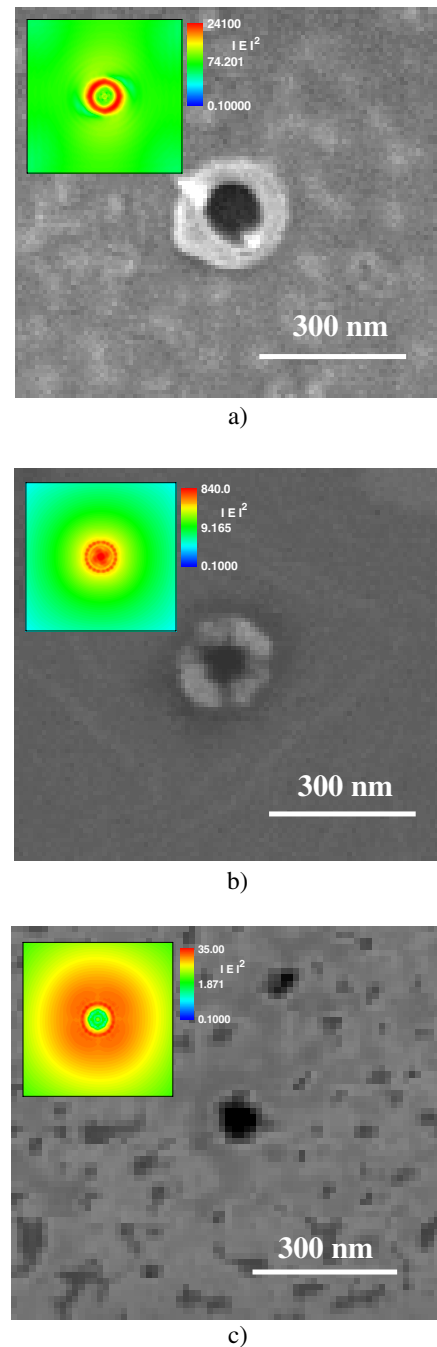
**Figure 2.** SEM images of holes produced in (a) Au, (b) Si and (c) SiO$_2$ substrates when the substrates with deposited nanoparticles are irradiated by a single laser shot. The applied laser fluence is 0.1, 0.13 and 6.3 J cm$^{-2}$, respectively. Laser radiation has circular polarization. The distribution of the near electric field intensity on the substrate surface calculated by FDTD simulation is also shown. The spatial scale of the intensity distribution is equivalent to the SEM image.

in the case of gold, where the electron–phonon relaxation time is as long as a few tens of ps [36]. The importance of thermal effects can be understood from the formation of the re-solidified rim around the holes in gold and silicon substrates, as is seen in SEM images shown in figure 2. The rim becomes more expressed with the increase of the applied laser fluence.

a)



b)



c)
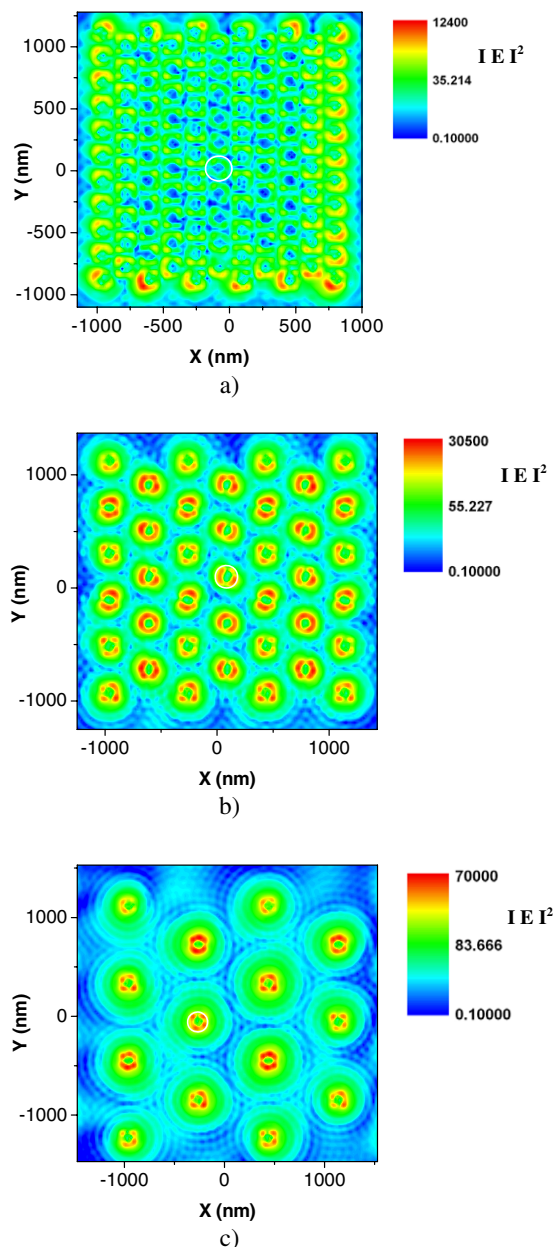
**Figure 3.** Calculated near electric field intensity distribution on gold substrate surface when gold nanoparticles with diameter of 200 nm are arrayed hexagonally and irradiated by electromagnetic waves at a wavelength of 800 nm. The field distribution is shown for three interparticle distances: (a) 200 nm (touching particles), (b) 400 nm and (c) 785 nm. The white line represents the particle delineation.

*Nanoparticle array*

Assuming a potential application of the enhanced near-field in the vicinity of gold nanoparticles to a reproducible technique for periodic surface nanostructuring, we will focus our further discussion on an arrayed particle system.

Figure 3 shows the electric near-field intensity distribution on the gold substrate surface on which gold nanoparticles with a diameter of 200 nm are arrayed hexagonally, and irradiated by laser pulses at wavelength of 800 nm. The intensity distribution is shown for the three interparticle
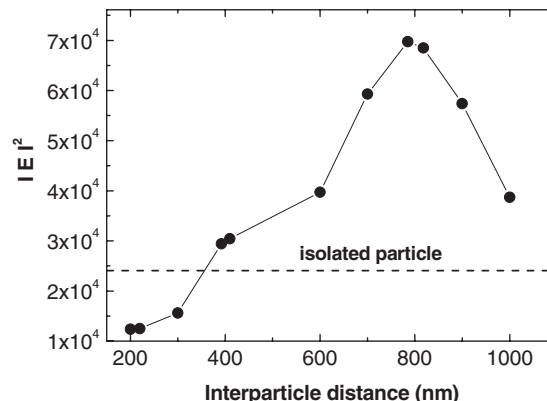


**Figure 4.** Dependence of the calculated maximal value of the near electric field intensity on the gold substrate on the interparticle distance. Dashed line shows the value for an isolated particle.

distances: (a) 200 nm (contact mode), (b) 400 nm and (c) 785 nm. The results indicate that the field intensity is enhanced under the particles, similarly to the case of the isolated particle one, but both the magnitude and the spatial distribution on the gold substrate surface are strongly dependent on the interparticle distance. The lowest value for the near-field intensity is achieved for the system of no interparticle distance (figure 3(a)). In this case the spatial distribution of the near-field intensity is not homogeneous, but the intensity is higher under the particles located at the edge of the aggregation, and it is about an order of magnitude lower than that under the particles located at the centre of the particle system. This intensity difference decreases with the increase of the interparticle distance, and in the case of 400 nm interparticle distance, the optical intensity distribution under all particles is similar. Furthermore, an increase in the near-field intensity with the increase of the interparticle distance is observed. In order to quantitatively express this tendency, a theoretical plot of the maximal value of the near electric field intensity distribution on the gold substrate as a function of the interparticle distance is shown in figure 4. The intensity for the isolated particle is also shown. The field intensity increases with the increase of the distance up to about 785 nm. This value becomes much higher than that of the isolated particle. A further increase of the interparticle distance up to 1000 nm results in a remarkable decrease of the maximal value of the field intensity.

The interparticle interaction can govern both the spatial distribution and the maximal strength of the electromagnetic field. Due to the capacitor effect a strong near-field strength can be developed in the interparticle gap of closely packed particles [12]. Thus, the properties of the near-field on the substrate are determined, not only by the interaction between the particle and its image charge on the substrate, as it is in the case of isolated particles, but also by the coupling between the neighbouring particles. The particle coupling effect is dependent on the interparticle distance and thereby this parameter will determine the near-field distribution and strength.

Figure 5 shows the results of the intensity distribution on an *yz* (cross-sectional) plane in the simulated system with gold substrate for three interparticle distances—(a) 200 nm (contact
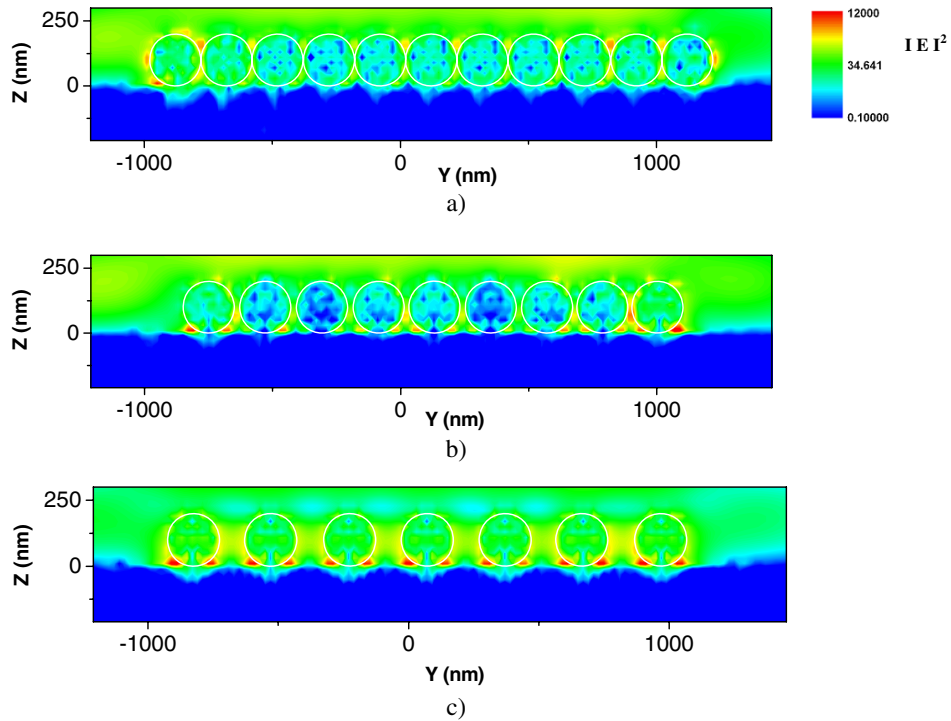
**Figure 5.** Electric field intensity distribution in an $yz$ plane of the simulation system with gold substrate for three interparticle distances:
(a) 200 nm (touching particles), (b) 220 nm and (c) 300 nm. The intensity distribution is shown in the plane that corresponds to a
cross-sectional view through the centre of a particle chain in the array structure. The particle chain is arbitrarily chosen, because the obtained
behaviour has similar features within the array. The substrate surface is at $z = 0$. The intensity colour scale in all figures is the same for clarity
in comparison. Particle delineations are shown by a white line.

mode), (b) 220 nm and (c) 300 nm. The intensity distribution is shown on the plane, corresponding to a cross-sectional view through the centre of a particle chain in the array structure. The particle chain is arbitrarily chosen, because the obtained behaviour has similar features within the arrays. It is seen that at the closest particle distance (figure 5(a)) the strongest field is achieved *between the particles*: the characteristic value is more than two times higher than the one obtained in the vicinity of the contact point between the particle and the substrate. With the increases of the interparticle distance the near-field coupling between the neighbouring particles becomes less efficient due to the evanescent character of the near-field. Here, the interaction between the image charges on the substrate surface and these induced on the particle surface becomes dominant for the near-field properties. In addition to the above discussion, we should mention that in the interaction between the optical radiation and small particles the characteristic absorption cross section of the particle can be several times larger than the geometrical size [37]. In a particle aggregate, this cross section is modified due to the presence of the neighbouring particles. The change of the interparticle distance will influence the absorption cross section and consequently the amplitude of the near electromagnetic field. This could explain the inhomogeneous near-field intensity distribution for the particles located at the edges of the aggregate and at its centre for an array consisting of closely spaced particles.

With the increase of the interparticle distance, the optical wave scattered by the particles also affects the near-field properties of the arrayed structure. It is shown previously that the local field of a particle array is governed by the retarded field of all assumed particles [11]. At a certain interparticle distance, when the radiative (not near-field) term is dominant, an increase and sharpening of the extinction peak can be realized. Such an effect could be expected when the interparticle distance approaches the incident wavelength and the diffracted field couples efficiently with the local plasmon of each particle. A periodically modified metal structure can satisfy the wave momentum conservation condition for the excitation of a surface plasmon wave. If we assume the present nanoparticle array on the gold substrate as a grating with a grating constant equal to the interparticle distance, then according to [38], the wavelength of the induced plasmon wave, $\lambda_{sp}$, is obtainable from the condition:

$$k_{sp} = k_0 \sin \theta_i \pm i k_{gx} \pm j k_{gy}, \qquad (1)$$

that gives for the diffraction order of ($i = 0$, $j = 1$) and at the normal incidence:

$$\lambda_{sp} = P \left( \frac{\varepsilon_m \varepsilon_1}{\varepsilon_m + \varepsilon_1} \right)^{\frac{1}{2}}. \qquad (2)$$

In the above equations, $k_{sp}$ is the wavevector of the air–gold surface plasmon mode, $k_0 \sin \theta_i$, is the in-plane wavevector of the incident wave, $\theta_i$ is the incident angle, $k_{gi}$ are the grating wavevectors, and $i$ and $j$ are integers. $P$ is the grating period, and $\varepsilon_m$ and $\varepsilon_1$ are the dielectric functions of gold and air, respectively. For the case of an interparticle distance of 785 nm (the interparticle distance corresponding to the highest
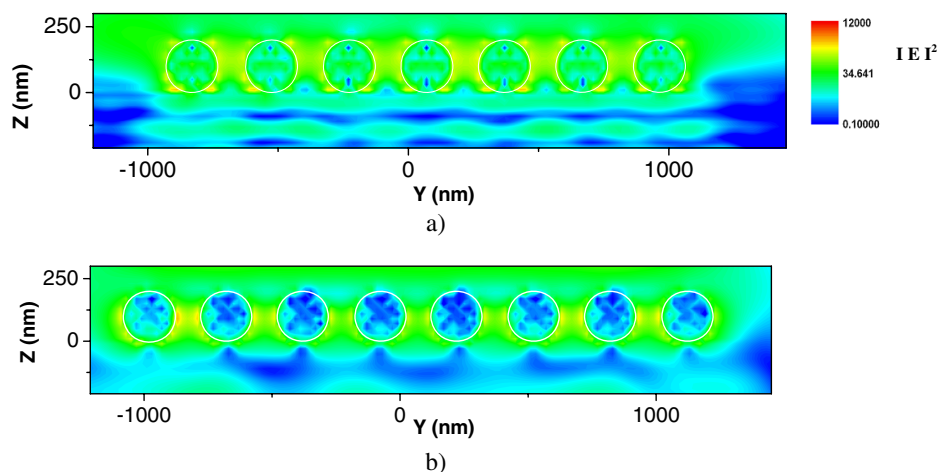
**Figure 6.** Intensity distribution in an $yz$ plane through the centre of a nanoparticle chain of the array on (a) silicon and (b) glass substrate when the interparticle distance is 300 nm. The intensity colour scale is the same for both figures as that for the case of gold substrate shown in figure 5(c) for clarity in comparison. The substrate surface is at $z = 0$. Particle delineations are shown by a white line.

field intensity obtained from FDTD simulation, as shown in figure 4) the plasmon wavelength calculated by equation (2) is consistent with the incident one. The resonance condition realized in this case can explain the maximal amplitude of the near electric field obtained at this distance. Decrease of the field enhancement value at larger interparticle spacing can be attributed to the out-of-phase interaction between the scattered optical field and the local plasmon of each particle and the higher losses of the optical field due to decrease of the particle density.

Although the particle distance influences the field distribution on the different substrates in a similar manner, the quantitative expression of the field properties is found to be different. Figure 6 shows the optical field intensity distribution in an $yz$ plane through the centre of a nanoparticle chain of the array for silicon (a), and glass substrate (b), when the interparticle distance is 300 nm. The intensity colour scale in the figures is the same as this for the case of gold substrate shown in figure 5(c) for clarity in comparison. It is seen that, while the maximal near-field intensity tends to be located in the vicinity of the contact point for the case of gold and silicon substrates (figures 5(c) and 6(a)), it is induced between the gold particles when glass substrate is considered at this interparticle distance.

A confirmation of the validity of the theoretical results is found experimentally. Figure 7 represents SEM images of the gold substrate before laser irradiation (a), and (b) after a single pulse irradiation at laser fluence of 0.15 J cm$^{-2}$. The spin-coating method used for deposition of the gold nanoparticles on the substrate leads to a random particle distribution, as single particles and clusters of different sizes are observed. After the laser irradiation single particles are removed from the surface and then holes can be seen in figure 7(b). The large clusters, however, remain on the substrate. According to the previously described near-field distribution properties, this selective particle removal and nanohole formation can be attributed to the lower field enhancement under the particle being composed of the closely packed array than the isolated (large distance
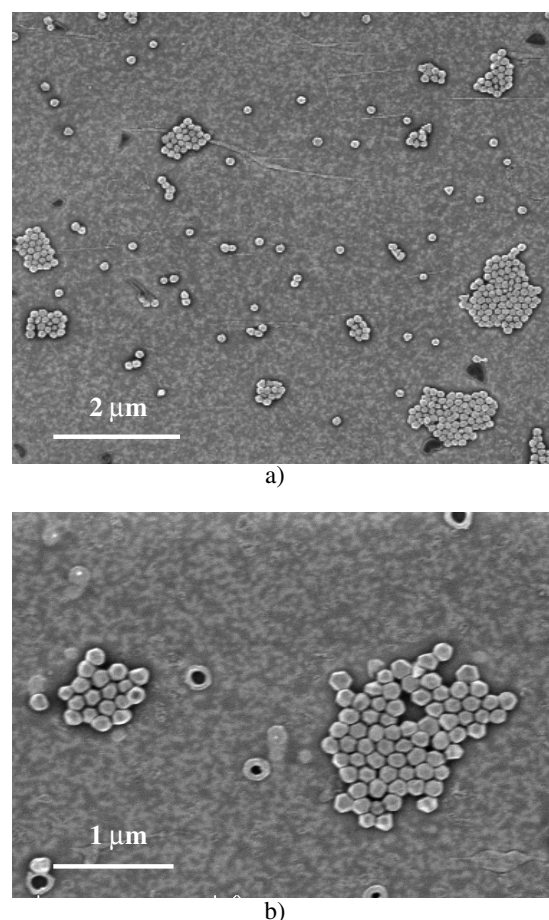


**Figure 7.** SEM images of the gold substrate (a) before laser irradiation and (b) after a single ultrashort pulse laser irradiation at a laser fluence of 0.15 J cm$^{-2}$.

separation) particles. Although the detailed explanation of the obtained phenomena will need more experimental verification, the present result confirms the validity of the theoretical findings. The obtained results will open a challenge for

further investigation in versatile applications of the near-field properties of arrayed nanoparticles that are in progress.

## 5. Conclusions

In this paper we present experimental and theoretical results on the near-field distribution in the vicinity of gold nanoparticles. The theoretical predictions of the existence of an enhanced near-field are confirmed experimentally: nanoholes are formed on different substrates after ultrashort laser irradiation of gold nanoparticles deposited on the substrate surface. As a function of the dielectric properties of the surroundings, the near-field characteristics are found to be different on the surface of Au, Si and SiO$_2$ substrates. The near-field intensity is maximal in the case of a metal substrate and lowest for a dielectric one. In all cases, the laser irradiation of the samples at fluences lower than the modification threshold of the native surface results in a formation of nanoholes with a size smaller than the gold nanoparticle diameter. The spatial distribution of the near-field on the substrate surface and quantitative difference of the field intensity for the different substrates predicted theoretically is confirmed by the experiment.

When a 2D nanoparticle array is considered, the near-field properties are found to strongly depend on the interparticle distance. In this configuration, the near-field distribution depends on the interaction between the charges of the neighbouring particles and those induced on the substrate surface. At interparticle distances smaller than the particle size the plasmon coupling leads to the localization of the highest intensity area between the particles. With the increase of the particle separation, this effect becomes less efficient and an area with the highest field enhancement is obtained in the vicinity of the contact point between the particle and the substrate. Increasing the interparticle distance a long range interaction mediated by a scattered optical field can affect the properties of the local field under the gold particles. These effects and their importance are found to depend on the substrate material.

The obtained results can be a base for the nanomodification technique of different optical and electronic materials. Furthermore, the present analyses can be used for an appropriate selection of substrate and interparticle distance in designing the efficient substrates for the surface-enhanced Raman scattering (SERS) technique.

## Acknowledgments

## References

[1]  Quinten M 2001 *Appl. Phys.* B **73** 245
[2]  El-Sayed M A 2001 *Acc. Chem. Res.* **34** 257
[3]  Klar T, Perner M, Grosse S, Von Plessen G, Spirkl W and Feldmann J 1998 *Phys. Rev. Lett.* **80** 4249
[4]  Quenten M, Leitner A, Krenn J R and Aussenegg F R 1998 *Opt. Lett.* **23** 1331
[5]  Maier S A, Kik P G, Atwater H A, Meltzer Sh, Harel E, Koel B E and Requicha A A G 2003 *Nat. Mater.* **2** 229
[6]  Leiderer P, Bartels C, König-Birk J, Mosbacher M and Boneberg J 2004 *Appl. Phys. Lett.* **85** 5370
[7]  Schnippering M, Carrara M, Foelske A, Kötz R and Fermin D J 2007 *Phys. Chem. Chem. Phys.* **9** 725
[8]  Quinten M 1995 *Z. Phys.* D **35** 217
[9]  Nedyalkov N N, Takada H and Obara M 2006 *Appl. Phys.* A **85** 163
[10]  Quinten M 2001 *Appl. Phys.* B **73** 245
[11]  Zou S, Janel N and Schatz G C 2004 *J. Chem. Phys.* **120** 10871
[12]  Felidj N, Aubard J, Levi G, Krenn J R, Schider G, Leitner A and Aussenegg F R 2002 *Phys. Rev.* B **66** 245407
[13]  Khlebtsov B, Zharov V, Melnikov A, Tuchin V and Khlebtsov N 2006 *Nanotechnology* **17** 5167
[14]  Kubik T, Bogunia-Kubik K and Sugisaka M 2005 *Curr. Pharm. Biotechnol.* **6** 17
[15]  Pissuwan D, Valenzuela S M and Cortie M 2006 *Trends Biotechnol.* **24** 62
[16]  Huang X, El-Sayed I H, Qian W and El-Sayed M A 2006 *J. Am. Chem. Soc.* **128** 2115
[17]  Schmidt J P, Cross S E and Buratto S K 2004 *J. Chem. Phys.* **121** 10657
[18]  Jersch J and Dickmann K 1996 *Appl. Phys. Lett.* **68** 868
[19]  Abe K, Hanada T, Yoshida Y, Tanigaki N, Takiguchi H, Nagasawa H, Nakamoto M, Yamaguchi T and Yase K 1998 *Thin Solid Films* **327** 524
[20]  Chen X Y, Li J R and Jiang L 2000 *Nanotechnology* **11** 108
[21]  Guan Y E and Pedraza A J 2005 *Nanotechnology* **16** 1612
[22]  Koch J, Korte F, Fallnich C, Ostendorf A and Chichkov B N 2005 *Opt. Eng.* **44** 051103
[23]  Juodkazis S, Nishimura K, Misawa H, Ebisui T, Waki R, Matsuo S and Okada T 2006 *Adv. Mater.* **18** 1361
[24]  Nakata Y, Okada T and Maeda M 2002 *Appl. Phys. Lett.* **81** 4239
[25]  Wang Z B, Hong M H, Luk'yanchuk B S, Lin Y, Wang Q F and Chong T C 2004 *J. Appl. Phys.* **96** 6845
[26]  Mosbacher M, Münzer H-J, Zimmermann J, Solis J, Boneberg J and Leiderer P 2001 *Appl. Phys.* A **72** 41
[27]  Brodoceanu D, Landström L and Bauerle D 2007 *Appl. Phys.* A **86** 313
[28]  Langer G, Brodoceanu D and Bauerle D 2006 *Appl. Phys. Lett.* **89** 261104
[29]  Taflove A and Hagness S C (ed) 2000 *Computational Electrodynamics: The Finite-Difference Time-Domain Method* (Boston, MA: Artech House)
[30]  Sendur K, Challener W and Peng C 2004 *J. Appl. Phys.* **96** 2743
[31]  Krug J T II, Sanchez E J and Xie X S 2002 *J. Chem. Phys.* **116** 10895
[32]  Laroche T and Girard Ch 2006 *Appl. Phys. Lett.* **89** 233119
[33]  Johnson P B and Christy R W 1972 *Phys. Rev.* B **6** 4370
[34]  Palik E D (ed) 1998 *Handbook of Optical Constants of Solids* (San Diego, CA: Academic Press)
[35]  Nedyalkov N, Sakai T, Miyanishi T and Obara M 2006 *J. Phys. D: Appl. Phys.* **39** 5037
[36]  Wellershoff S-S, Hohlfeld J, Güdde J and Matthias E 1999 *Appl. Phys.* A **69** S99
[37]  Wang Z B, Luk'yanchuk B S, Hong M H, Lin Y and Chong T C 2004 *Phys. Rev.* B **70** 035418
[38]  Ghaemi H F, Thio T, Grupp D E, Ebbesen T W and Lezec H J 1998 *Phys. Rev.* B **58** 6779